AIP | Applied Physics Letters

Formation of Ru nanocrystals by plasma enhanced atomic layer deposition for nonvolatile memory applications

Sung-Soo Yim, Moon-Sang Lee, Ki-Su Kim, and Ki-Bum Kim

Citation: Applied Physics Letters **89**, 093115 (2006); doi: 10.1063/1.2338793
View online: http://dx.doi.org/10.1063/1.2338793
View Table of Contents: http://scitation.aip.org/content/aip/journal/apl/89/9?ver=pdfcov
Published by the AIP Publishing

Articles you may be interested in

Charge trapping characteristics of Au nanocrystals embedded in remote plasma atomic layer-deposited Al2O3 film as the tunnel and blocking oxides for nonvolatile memory applications
J. Vac. Sci. Technol. A **30**, 01A104 (2012); 10.1116/1.3639131

Nonvolatile memory characteristics of atomic layer deposited Ru nanocrystals with a SiO 2 / Al 2 O 3 bilayered tunnel barrier
J. Appl. Phys. **107**, 013707 (2010); 10.1063/1.3275346

Development of plasma-enhanced atomic layer deposition grown Ru–WCN mixed phase films for nanoscale diffusion barrier and copper direct-plate applications
J. Vac. Sci. Technol. B **27**, 631 (2009); 10.1116/1.3097856

Application of plasma enhanced chemical vapor deposition silicon oxynitride layers in nonvolatile semiconductor memory devices
J. Vac. Sci. Technol. B **27**, 494 (2009); 10.1116/1.3054353

Evaluation of integrity and barrier performance of atomic layer deposited W N x C y films on plasma enhanced chemical vapor deposited Si O 2 for Cu metallization
Appl. Phys. Lett. **89**, 081913 (2006); 10.1063/1.2338768

This article is copyrighted as indicated in the article. Reuse of AIP content is subject to the terms at: http://scitation.aip.org/termsconditions. Downloaded to IP: 120.117.138.77 On: Thu, 27 Nov 2014 04:04:20

APPLIED PHYSICS LETTERS **89**, 093115 (2006)

Formation of Ru nanocrystals by plasma enhanced atomic layer deposition for nonvolatile memory applications

Sung-Soo Yim, Moon-Sang Lee, Ki-Su Kim, and Ki-Bum Kim[a)]
School of Materials Science and Engineering, Seoul National University, Seoul 151-742, Korea

(Received 26 May 2006; accepted 3 July 2006; published online 30 August 2006)

The formation of Ru nanocrystals is demonstrated on a SiO_2 substrate by plasma enhanced atomic layer deposition using diethylcyclopentadienyl ruthenium and NH_3 plasma. The island growth of Ru was observed at the initial stages of the film formation up to a nominal thickness of 11.1 nm. A maximum Ru nanocrystal spatial density of 9.7×10^{11} /cm^2 was achieved with an average size of 3.5 nm and standard deviation of the size of 20%. Electron charging/discharging effect in the Ru nanocrystals is demonstrated by measuring the flatband voltage shift in the capacitance-voltage measurement of metal-oxide-semiconductor memory capacitor structure. © *2006 American Institute of Physics*. [DOI: 10.1063/1.2338793]

Memory device structures with nanocrystal (or quantum dot) floating gates have been considered as a possible solution for the next generation of nonvolatile memory devices.[1] However, for the integration of nanocrystals into the memory device structure, it is important to develop a reproducible deposition method which guarantees the simultaneous control of the spatial density, size, and size distribution of the nanocrystals. Recently, direct deposition utilizing an initial stage of chemical vapor deposition (CVD),[2–4] a thermally induced self-organization process by precipitation of implanted ions,[5,6] or the agglomeration of physical vapor deposited thin metal films[7,8] has been widely investigated for nanocrystal formation. Among these processes, the low pressure CVD (LPCVD) of Si has been found to offer relatively good controllability of both the size and spatial density of the nanocrystals and, thus, is widely employed as one of the most promising process technologies to form nanocrystals.[9] However, the control of nucleation and growth at the initial stages of CVD appears to remain a very difficult problem, because complicated chemical reactions such as decomposition, physisorption, chemisorption, and the surface reactions of the introduced precursor/reactant molecules occur simultaneously within a short deposition time (typically less than 1 min in the LPCVD system). Also, the film growth which results from combinations of various process parameters such as the temperature, precursor/reactant ratio, and pressure of the precursor/reactant is too difficult to control.

Atomic layer deposition (ALD), on the other hand, uses a self-limiting film growth mechanism caused by surface saturated reactions through the sequential exposure of the precursor and reactant at each ALD cycle.[10] One ALD cycle typically consists of precursor pulsing for precursor adsorption, purging of the physisorbed precursors, reactant pulsing for surface reaction, and purging of the by-product. Therefore, the ALD process appears to have the following advantages over the conventional CVD process in terms of its ability to control thin film formation processes. First, the deposition conditions can be precisely controlled by making independent adjustments of the process parameters at each subcycle stage. Second, the deposition time can be digitally controlled by adjusting the number of ALD cycles. Third, the growth rate (or equivalently the adatom flux) is relatively independent of process variables such as the temperature and precursor/reactant ratio and can be controlled simply by adjusting the precursor dose. In particular, the purging stage can play the role of shifting the deposition process close to the equilibrium condition by offering more free time for the surface diffusion of the deposited adatoms. This means that the deposited adatoms have more chance to seat on the energetically stable sites without being disturbed by unwanted species such as the physisorbed precursors and by-products of the reaction. Therefore, the ALD process can be a more useful process for depositing uniform nanocrystals in specific deposition systems such as that involving the formation of metal nanocrystals on a dielectric substrate, which generally tends to lead to island growth. Herein, we demonstrate that the ALD process can be a facile route to uniform nanocrystal deposition by using the plasma enhanced ALD (PEALD) of Ru as an example.

The ALD of Ru has been studied for applications involving a glue layer for Cu electrodeposition,[11] electrodes for dynamic random access memory capacitors,[12] and metal gates for complementary metal-oxide semiconductor.[13] It has been reported that the ALD of Ru on dielectric substrates shows a substantial incubation period, which indicates the possibility of having a large process window for island growth.[14] In addition, the PEALD process can be used to modify the nucleation stage. Recently, Kwon *et al.* reported that the PEALD Ru process on TiN shows no apparent incubation period. This result implies that the nucleation rate is significantly enhanced by the PEALD process.[11] Another reason for selecting Ru is its high chemical and thermal stability, which is compatible with current semiconductor technology. The relatively large work function (4.7 eV) of Ru is also advantageous for the application of this material to nanocrystal floating gate memory devices, because this would be expected to give rise to better retention and charging effectiveness.[7]

Ru nanocrystals were deposited on thermally grown SiO_2 (100 nm)/Si (100) substrates using a showerhead-type GENI-MP1000 PEALD system (ASM-Genitech, Inc.) at a deposition temperature of 300 °C and total pressure of 3 Torr. Ar (99.999%) gas was used as both a carrier gas and purging gas. Diethylcyclopentadienyl ruthenium

---

[a)]Electronic mail: kibum@snu.ac.kr

This article is copyrighted as indicated in the article. Reuse of AIP content is subject to the terms at: http://scitation.aip.org/termsconditions. Downloaded to IP: 120.117.138.77 On: Thu, 27 Nov 2014 04:04:20

0003-6951/2006/89(9)/093115/3/$23.00

© 2006 American Institute of Physics

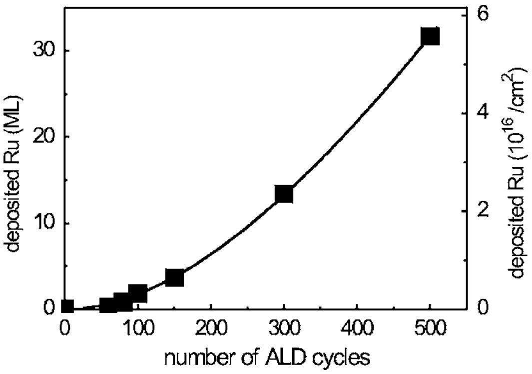

FIG. 1. Number of deposited Ru on SiO_2 as a function of the ALD cycles.

($Ru(EtCp)_2$) (99.60%) vapor was generated in a bubbler at 80 °C, at which the saturated vapor pressure of $Ru(EtCp)_2$ is 0.18 Torr, and carried into the process chamber by Ar at a flow rate of 100 sccm (standard cubic centimeter per minute). An rf plasma of NH_3 (99.999%) diluted by Ar was used as a reducing agent. The flow rates of NH_3 during pulsing and Ar during purging were both 150 sccm. One ALD cycle consisted of $Ru(EtCp)_2$ pulsing, purging, NH_3 plasma treatment at a rf power of 100 W, and purging for durations of 5, 5, 15, and 3 s, respectively. To determine the optimal pulsing times affording self-limited growth, the pulsing times of $Ru(EtCp)_2$ and NH_3 were independently varied. The nominal growth rate of Ru was saturated at 0.025 nm/cycle when the $Ru(EtCp)_2$ and NH_3 pulsing times exceeded 5 and 10 s, respectively. The spatial density, average size, size distribution, and average height of Ru as a function of the number of ALD cycles were measured using plan-view and cross-sectional transmission electron microscopy (TEM) (JEOL JEM-3000F with a field emission gun operated at 300 kV) and scanning electron microscopy (JEOL JSM 7401F). The resistivity of the 25 nm thick Ru film was about 35 $\mu\Omega$ cm. Capacitance-voltage (C-V) measurement was conducted using an Agilent 4284A precision *LCR* meter.

Figure 1 shows the number of Ru atoms deposited as a function of the number of ALD cycles. The number of Ru atoms deposited for less than 300 ALD cycles was calculated from the molar volume of bulk Ru (8.17 mole/cm^3) and the average volume of the nanocrystals, which was estimated from their average size and height in the plan-view and cross-sectional TEM micrographs assuming that they have a spherical shape. The number of Ru atoms corresponding to 1 ML is defined as 1.76×10^{15} atoms/cm^2, which is calculated from the molar volume to the power 2/3. From 300 ALD cycles, where the Ru islands start to agglomerate, the number of deposited Ru atoms is calculated from the surface coverage and nominal thickness. As shown in Fig. 1, the trend between the amount of Ru deposited and the number of ALD cycles shows a nonlinear relationship below 500 ALD cycles, unlike ideal ALD growth behavior. Recent studies have revealed that the difference in the probabilities of the precursor being adsorbed on the deposited material and substrate is the reason for the nonlinear growth behavior in the initial stages of ALD.[15] From the analyses of Puruunen[15] and Lim *et al.*[16] the number of atoms deposited per cycle can be calculated from the probabilities of the Ru precursor being adsorbed on Ru, α, and SiO_2, β. In our case, the number of atoms deposited per cycle is defined as

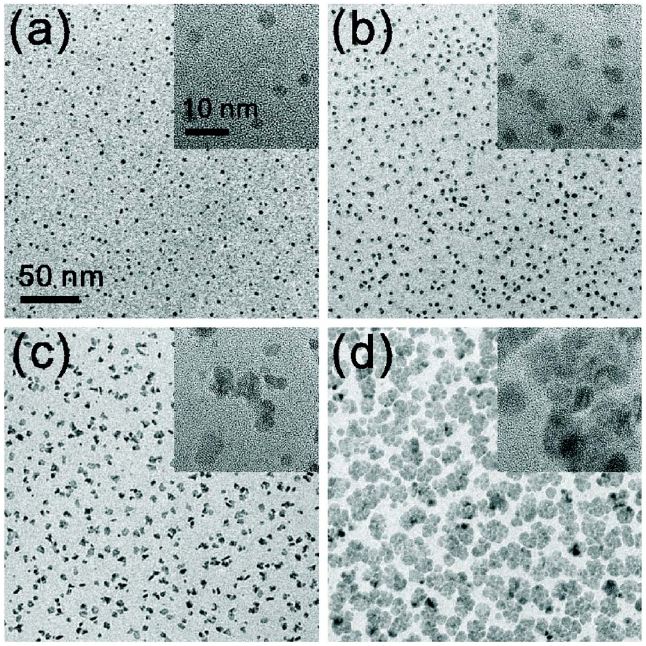

FIG. 2. Plan-view TEM micrographs of Ru nanocrystals deposited for 100 (a), 200 (b), 300 (c), and 500 (d) ALD cycles. The inset figures are HRTEM images of the corresponding cycles.

$$f(n) = k\alpha - k(\alpha - \beta)(1 - \beta)^{n-1}, \tag{1}$$

where $f(n)$ is the number of atoms deposited at the nth ALD cycle and k is the conversion factor from the surface coverage to the number of atoms. Using this model, it is found that the adsorption probability of the Ru precursor on Ru is about 270 times larger than that on the SiO_2 substrate. The line in Fig. 1 shows the fitting lines derived from this model, which shows a good match with the experimental results.

Figure 2 shows the bright-field plan-view TEM micrographs of the Ru nanocrystals deposited on SiO_2 after 100 (a), 200 (b), 300 (c), and 500 (d) ALD cycles. The inset shows the high resolution TEM (HRTEM) micrographs of the corresponding samples. Below 200 ALD cycles, the formation of discrete and circular nanocrystals on SiO_2 with good spatial and size uniformity is observed [Figs. 2(a) and 2(b)]. The coalescence of the Ru nanocrystals occurs after 200 ALD cycles, as shown in Figs. 2(c) and 2(d). It is noted that Ru forms islands even at 500 ALD cycles [Fig. 2(d)], which corresponds to a nominal thickness of 11.1 nm. It is considered that this wide process window for the island growth of PEALD Ru on SiO_2 comes from the preferential deposition of Ru on the preformed nuclei. In addition, the wetting angle between Ru and SiO_2 is expected to be close to 180°, due to the large difference in surface energies [3.0 J/m^2 for Ru (Ref. 17) and 0.2 J/m^2 for SiO_2 (Ref. 18)] and negligible interface energy between Ru and SiO_2. Thus, this large wetting angle causes the ALD system of Ru on SiO_2 to have a greater tendency toward island growth.

Figure 3 shows the spatial density and average size of the Ru nanocrystals deposited on SiO_2 as a function of the number of ALD cycles. The spatial density of the nanocrystals was measured by counting the number of Ru nanocrystals in the plan-view TEM images. The spatial density of the Ru nanocrystals increases in the early stages of ALD, shows a maximum density of 9.7×10^{11} /cm^2 at 200 ALD cycles, and then decreases due to the coalescence of the Ru nano-

This article is copyrighted as indicated in the article. Reuse of AIP content is subject to the terms at: http://scitation.aip.org/termsconditions. Downloaded to IP: 120.117.138.77 On: Thu, 27 Nov 2014 04:04:20

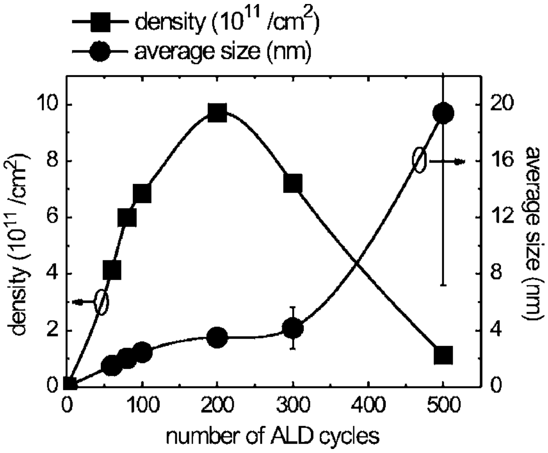

FIG. 3. Spatial density and average size of Ru nanocrystals as a function of the ALD cycles.

crystals. The average size of the nanocrystals increases linearly from 1.5 nm at 60 ALD cycles to 3.5 nm at 200 ALD cycles, before the coalescence of the Ru nanocrystals occurs. After 200 ALD cycles, the average size and its deviation increase steeply due to the coalescence of the Ru nanocrystals. While it is not shown in the data, it is noted that the standard deviation of the nanocrystal size is measured to be about 20%, below 200 ALD cycles.

We made metal-oxide-semiconductor (MOS) capacitor embedded with Ru nanocrystals deposited for 200 ALD cycles for the confirmation of electron charging/discharging effects in Ru nanocrystals. Tunnel oxide of 5 nm thickness was thermally grown on *n*-type Si substrate using a rapid thermal process. After Ru deposition, 25 nm thick control oxide was deposited by plasma enhanced chemical vapor deposition. Finally, Al top gate was deposited by thermal evaporation and patterned by photolithography. Figure 4 shows the high frequency *C*-*V* characteristics of MOS capacitor with Ru nanocrystals after voltage sweeping between ∓ 2, ∓ 6, and ∓ 10 V. The flatband voltage shift (ΔV_{FB}) gradually increases as the voltage sweep range increases. Large ΔV_{FB} of 3.6 V during backward sweep and 3.1 V during forward sweep are achieved at the sweep range between ∓ 10 V, while negligible ΔV_{FB} (<0.01 V) was observed for MOS capacitor without Ru nanocrystals. It is worth noting that more enhanced retention characteristics of the present Ru nanocrystals could be expected from the asymmetric charging/discharging behavior because electrons should overcome large tunnel barrier for discharging process. This asymmetric charging process can also be expected from the large work function of Ru (4.7 eV).

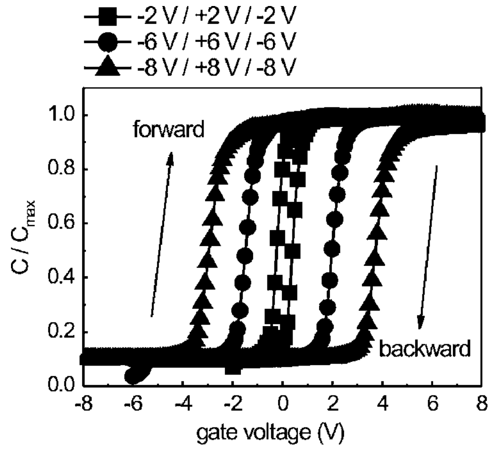

FIG. 4. High frequency *C*-*V* characteristics for a MOS capacitor with the Ru nanocrystal floating gate.

In summary, we demonstrate that a uniform nanocrystal array with a high spatial density and narrow size distribution can be deposited using the Ru PEALD process. The large difference in adsorption probabilities of Ru precursors on between Ru and SiO_2 and the large difference in surface energies of Ru and SiO_2 are thought to be responsible for the large process windows for island growth of the presented method. Ru nanocrystals with an average size of 3.5 nm and size deviation of 20% are incorporated into MOS-type memory structures.

This work was supported by the National Program for Tera-Level Nano Devices, one of the Frontier R&D Programs funded by the Ministry of Science and Technology of Korea.. The authors also acknowledge that part of the funding came from the National Core Research Center (NCRC) program through the NANO Systems Institute and BK-21 program through the Ministry of Education of Korea.

[1] A. Thean and J.-P. Leburton, IEEE Potentials **21**, 35 (2002).

[2] R. Muralidhar, R. F. Steimle, M. Sadd, R. Rao, C. T. Swift, E. J. Prinz, J. Yater, L. Grieve, K. Harber, B. Hradsky, S. Straub, B. Acred, W. Paulson, W. Chen, L. Parker, S. G. H. Anderson, M. Rossow, T. Merchant, M. Paransky, T. Huynh, D. Hadad, Ko-Min Chang, and B. E. White, Jr., Tech. Dig. - Int. Electron Devices Meet. **2003**, 26.2.1.

[3] S. J. Baik, S. Choi, U.-I. Chung, and J. T. Moon, Tech. Dig. - Int. Electron Devices Meet. **2003**, 22.3.1.

[4] B. De Salvo, C. Gerardi, S. Lombardo, T. Baron, L. Perniola, D. Mariolle, P. Mur, A. Toffoli, M. Gely, M. N. Semeria, S. Deleonibus, G. Ammendola, V. Ancarani, M. Melanotte, R. Bez, L. Baldi, D. Corso, I. Crupi, R. A. Puglisi, G. Nicotra, E. Rimini, F. Mazen, G. Ghibaudo, G. Pananakakis, C. M. Compagnoni, D. Ielmini, A. Lacaita, A. Spinelli, Y. M. Wan, and K. van der Jeugd, Tech. Dig. - Int. Electron Devices Meet. **2003**, 26.1.1.

[5] H. I. Hanafi, S. Tiwari, and I. Khan, IEEE Trans. Electron Devices **43**, 1553 (1996).

[6] E. Kapetanakis, P. Normand, D. Tsoukalas, K. Beltsios, J. Stoemenos, S. Zhang, and J. van den Berg, Appl. Phys. Lett. **77**, 3450 (2000).

[7] Z. Liu, C. Lee, V. Narayanan, G. Pei, and E. C. Kan, IEEE Trans. Electron Devices **49**, 1606 (2002).

[8] J. J. Lee, Y. Harada, J. W. Pyun, and D.-L. Kwong, Appl. Phys. Lett. **86**, 103505 (2005).

[9] F. Mazen, T. Baron, J. M. Hartmann, M. N. Semeria, and G. Brémond, Mater. Res. Soc. Symp. Proc. **737**, F.1.9.1 (2003).

[10] M. Leskela and M. Ritala, Thin Solid Films **409**, 138 (2002).

[11] O.-K. Kwon, S.-H. Kwon, H.-S. Park, and S.-W. Kang, J. Electrochem. Soc. **151**, C753 (2004).

[12] J. Lin, T. Suzuki, D. Matsunaga, and K. Eguchi, Appl. Phys. Lett. **88**, 062902 (2006).

[13] M. Tapajna, P. Pısecny, R. Luptaka, K. Husekova, K. Frohlich, L. Harmatha, J. C. Hooker, F. Roozeboom, and J. Jergel, Mater. Sci. Semicond. Process. **7**, 271 (2004).

[14] T. Aaltonen, P. Alen, M. Ritala, and M. Leskela, Chem. Vap. Deposition **9**, 45 (2003).

[15] R. L. Puruunen, J. Appl. Phys. **95**, 4777 (2004).

[16] J.-W. Lim, H.-S. Park, and S.-W. Kang, J. Appl. Phys. **88**,6327 (2000).

[17] W. R. Tyson and W. A. Miller, Surf. Sci. **62**, 267 (1977).

[18] R. K. Iler, *The Chemistry of Silica* (Wiley, New York, 1979), pp. 645–647.

This article is copyrighted as indicated in the article. Reuse of AIP content is subject to the terms at: http://scitation.aip.org/termsconditions. Downloaded to IP: 120.117.138.77 On: Thu, 27 Nov 2014 04:04:20